

Published in final edited form as:

Cardiol Clin. 2013 May ; 31(2): . doi:10.1016/j.ccl.2013.03.001.

Anatomy of the Mitral Valve Apparatus – Role of 2D and 3D Echocardiography

Jacob P. Dal-Bianco, MD and

Instructor in Medicine, Massachusetts General Hospital, Harvard Medical School, 55 Fruit Street, Yawkey 5B, Boston, MA, 02114, Office tel: 617 643 0165, Office fax: 617 643 3963

Robert A. Levine, MD

Professor of Medicine, Massachusetts General Hospital, Harvard Medical School, Cardiac Ultrasound Laboratory, 55 Fruit Street, Yawkey 5E, Boston, MA, 02114, Office tel: 617 724 1995, Office fax: 617 643 1616

Jacob P. Dal-Bianco: jdalbiano@partners.org; Robert A. Levine: rlevine@partners.org

Abstract

The mitral valve apparatus is a complex three-dimensional functional unit that is critical to unidirectional heart pump function. This review details the normal anatomy, histology and function of the main mitral valve apparatus components 1) mitral annulus, 2) mitral valve leaflets, 3) chordae tendineae and 4) papillary muscles. 2 and 3 dimensional Echocardiography is ideally suited to examine the mitral valve apparatus and has provided insights into the mechanism of mitral valve disease. An overview of standardized image acquisition and interpretation is provided. Understanding normal mitral valve apparatus function is essential to comprehend alterations in mitral valve disease and the rationale for repair strategies.

Keywords

mitral valve apparatus; mitral valve; mitral annulus; papillary muscles; chordae tendineae; mitral regurgitation; echocardiography

Introduction

The normal mitral valve apparatus is a dynamic three-dimensional system that allows brisk left ventricular (LV) blood-inflow during diastole and ensures unidirectional heart pump function by sealing the left atrium from the LV during systole. Key components are the mitral annulus, the mitral valve leaflets, the chordae tendineae, and the LV wall with its attached papillary muscles (PMs) (Figure 1). Proper valve function is dependent on the integrity and harmonious interplay of these components – and an imbalance can result in a leaking (regurgitant, insufficient, incompetent), stenotic, or combined regurgitant and stenotic valve dysfunction. A detailed understanding of mitral valve apparatus development, anatomy and function is important for cardiac imaging interpretation, for disease diagnosis, and comprehending the rationale for repair strategies. Repair of the diseased mitral valve

© 2013 Elsevier Inc. All rights reserved.

Financial Disclosure: The authors have nothing to disclose.

Publisher's Disclaimer: This is a PDF file of an unedited manuscript that has been accepted for publication. As a service to our customers we are providing this early version of the manuscript. The manuscript will undergo copyediting, typesetting, and review of the resulting proof before it is published in its final citable form. Please note that during the production process errors may be discovered which could affect the content, and all legal disclaimers that apply to the journal pertain.

requires understanding the *dysfunction* caused by the disease *lesion* in order to restore a normally functioning valve, a lesson learned from one of the foremost pioneer's in mitral valve repair – Prof. Alain Carpentier.

Mitral Valve Apparatus Development

Mitral valve development is complex and still under investigation (1). The developing heart tube consists of extracellular matrix sandwiched by myocardial and endothelial layers, and has folded into a basic four-chamber configuration by the end of fetal week 4. By week 5 the outer myocardial layer has compacted and trabecular structures start to form within the future LV cavity. At this point, superior, inferior and lateral cardiac cushions can be detected in the common atrioventricular (AV) canal (2). These 5 cushions are formed by endothelial cells that migrate into the mesenchyme and change into an interstitial fibroblasts cell-type, a process termed endothelial–mesenchymal transdifferentiation or transformation (EMT) (1). The superior and inferior cardiac cushions fuse at week 7 to 7 ! and divide the common AV canal into right and left portions. The anterior (aortic) leaflet of the mitral valve originates from the fused superior and inferior cushion tissue in the left AV canal and starts to delaminate or separate from the myocardial wall shortly thereafter. The posterior (mural) leaflet forms from the left lateral cushion (2). Over weeks 8–10 the LV intracavitary trabecular bridges compact, and by week 10 small (antero)lateral and (postero)medial papillary muscles (PMs) can be observed delaminated in the LV cavity. Actually both are located posteriorly relative to the anterior chest wall - one medial, the other lateral. Both PMs attach directly to both leaflet-forming cushions. From week 11 to 13 the leaflets continue to form, the PMs become more distinct, and rudimentary chordae develop. By week 15 the MV leaflets, chordae and PMs become developed (2). The mitral valve apparatus then continues to grow to meet the needs and demands of the developing organism (3).

Mitral Valve Apparatus Anatomy & Histology

1) Mitral annulus

The mitral annulus (MA) is defined by the tissue juncture of the left atrium, the left ventricle and the mitral leaflets. It is a dynamic, anatomically ill-defined structure. En face the MA resembles a kidney-bean; in three dimensions it is a non-planar saddle shape (4–6).

The anterior flatter portion of the mitral annulus is continuous with the aortic annulus, is the elevated (most atrial) “horn” of the saddle shape and consists of parallel collagen fibers (4,7). The MA-to-aortic annular angle changes dynamically over the cardiac cycle, with displacement coupled through the fibrous continuum (8). Reciprocal systolic and diastolic aortic and mitral annulus area changes have been observed (9–11). The posterior part of the MA runs distal to the left (lateral) and right (medial) fibrous trigones and includes the low points of the saddle close to the lateral and medial commissures and the posterior saddle horn. Compared to the anterior portion, the posterior mitral annulus is more loosely anchored to the surrounding tissue, allowing it to move freely with myocardial contraction and relaxation (7). It is basically a junction of leaflet and myocardium. Less static in all dimensions than the anterior MA portion, the posterior MA allows for systolic apical bending along a mediolateral commissure axis, with increased saddle height and circumferential area decrease (12). The saddle-shaped MA and its dynamic change reduces leaflet tissue stress and is important for coaptation geometry (13–20). The MA is innervated and supplies blood vessels to the leaflets (21–23). From week 18 to 24 on to adulthood the MA area increases 25-fold (24) and, contrary to the widely published “normal” mitral annular orifice area of 4–6cm², multiple investigations with differing imaging modalities report an average mitral annular area of ~10cm² in healthy subjects (25–30). MA area can

significantly increase in patients with dilated LVs (27,29,30). This is accompanied by MA flattening (29,31) and decrease and delay of systolic sphincter-like mitral annular area reduction (29,32). The final result of these changes is altered leaflet stress and unfavorable mitral leaflet remodeling (Table 1). MA flattening has also been recently described in myxomatous valve disease, associated with more severe MR and chordal rupture, potentially related to increased out-of-plane stresses (20,33).

2) Mitral valve leaflets

The mitral valve has anterior and posterior leaflets and variable commissural scallops to occlude medial and lateral gaps (Figure 1C, Figure 2). Leaflet tissue circumferentially attaches to the mitral annulus with a minimum tissue length of 0.5 to 1cm (34). Redundant leaflet tissue is critically important for leaflet apposition and tight leaflet coaptation. In normal and dilated LVs a leaflet to MA area ratio of 1.5 to 2 has been found sufficient to prevent significant mitral regurgitation (30,34). The atrial surface of the leaflets is smooth and the leaflet body translucent (Figure 2). A hydrophilic protein rich zone, termed rough zone, starts ~1 cm from the distal leaflet edge. When the leaflets coapt, the irregular, soft surface of this zone helps to maintain and insure a seal (Figure 2, Coaptation zone). The ventricular surface of especially the anterior leaflet is a basket-weave of criss-crossed collagen strands that originate at the chordal insertion and continue into the annulus (35,36). Secondary chordae insert close to the rough zone, while primary chordae insert at the free leaflet tips (35,37).

The anterior (also labeled aortic or septal) mitral leaflet is trapezoid- or dome-shaped, anchored to the fibrous portion of the mitral annulus, and shares a fibrous tissue continuity mainly with the noncoronary cusp of the aortic valve (Figure 2). Its collagen fiber orientation suggests tight anchoring into the left (anterolateral) and right (posteromedial) fibrous trigones (38). The anterior leaflet is larger, longer and thicker than the posterior leaflet (Table 2, Figure 2). To facilitate diagnostic and therapeutic medical communication, the anterior leaflet can be divided into lateral (A1), central (A2) and medial scallops (A3). For the anterior leaflet, this nomenclature does not represent anatomically distinct structures (Figure 1C).

The posterior (mural) leaflet is crescentic with a long circumferential base (~5cm vs ~3cm anterior leaflet, (39)) and relatively short radial length (Figure 1C and Figure 2; Table 1). It is attached to the posterior portion of the mitral annulus. Similar to the anterior leaflet, the posterior leaflet can be divided into lateral (P1), central (P2) and medial scallops (P3). Slits and indentations within the posterior mitral tissue demarcate these scallops (Figure 1C) (37).

Additional leaflet tissue termed commissural, accessory or junctional can be found at the anterolateral (A1-P1) and posteromedial (A3-P3) commissures (Figure 1B and 1C, Figure 2). Their tissue length measured from annular insertion varies from 0.5 to 1cm. (34,35).

The MV leaflets fully open in less than 100ms 3 billion times throughout a lifetime and are exposed to a wide range of LV pressures (40). Despite this demanding environment, significant MV disease is uncommonly seen in patients younger than 65 years (41). Influenced by the immediate environment and mechanical needs, the MV leaflet tissue is trilaminar, consisting of fibrosa/ventricularis, spongiosa and atrialis layers. Valvular endothelial cells cover the blood-interfacing surfaces. Each layer has unique extracellular matrix (ECM) characteristics: Hemodynamically exposed to LV pressures, the fibrosa/ventricularis is composed of dense collagen, which is important for mechanical stability. The spongiosa has less organized collagen, but especially at the leaflet tip rough zone, is rich in water absorbent proteins. This protects the leaflet edges and ensures a tight seal. The atrialis contains a network of collagen and elastin and appears to play a critical role in leaflet

remodeling and adaptation (42). While trilaminar, the layer distribution of the anterior and posterior leaflets differs significantly: Much of the anterior leaflet thickness is due to a dominant fibrosa layer, which allows this leaflet to withstand a significantly higher tensile load without tissue disruption. The posterior leaflet is thinner and more flexible (43,44). The anterior mitral leaflet has an especially dense innervation, and nerve terminals close to smooth muscle cells and fibroblasts suggest a potential neural feedback or regulatory mechanism (45). Interestingly, but of unknown significance, this neural innervation greatly diminishes with age (45,46). Cardiac muscle cells can be detected in both leaflets close to the annulus. This tissue is excitable via the atria, isolated from LV excitation, and resembles atrial myocardium (36). The healthy, mature MV has a very rudimentary vascular and lymphatic system (23,47), interstitial cells are mostly dormant, and the ECM turnover is slow. Physiologic or pathologic-induced leaflet stress can induce prominent EMT, interstitial cell activation & proliferation, ECM remodeling and neovascularization (3,42,48,49). Regulation of mitral leaflet adaptation is not well understood, but the wide range of total leaflet area (Table 2) suggests a potent adaptation mechanism that has to be further explored and therapeutically targeted.

3) Chordae tendineae

The chordae tendineae are fibrous strings that originate with highly variable branching from the PM tips (heads) and insert fan-like into the ventricular aspects of the anterior, posterior and commissural leaflets (Figure 1B and 1C, Figure 2) (37,50). Occasionally chordae originate from the basal posterior myocardium and insert directly into the posterior leaflet (34). Two main types of chordae can be distinguished based on leaflet insertion: Primary (marginal) chordae, which attach to the leaflet free edges, and secondary (basal) chordae which insert into the anterior leaflet edge rough zone and throughout the posterior leaflet body (51). Chordae are composed of an interfacing, tightly linked collagen and elastin network that dampens PM-leaflet force transmission (50).

Secondary chordae are thicker than primary chordae and have more tightly crimped collagen, making them more extensible (52). Commonly a pair of thick secondary chordae, termed strut chordae, insert at 4 and 8pm into the ventricular aspect of the anterior leaflet; additional strut chords, including to the posterior leaflet have been described. Basket-woven collagen fibers distribute chordal force over the leaflet surface from insertion to the annulus (34,36,51). To relieve pathologic apical leaflet tethering and restore mitral leaflet coaptation in patients with functional/ischemic mitral regurgitation, selected secondary chordae can be cut without deleterious effects on LV function (53–55).

Primary chordae are thinner, insert at the leaflet tips and have limited extensibility due to higher collagen fibril density and reduced crimping (52). These characteristics prevent leaflet edge eversion (=flail leaflet) (56). There is a wide variability in chordal anatomy and branching patterns (37) which makes correct anatomic labeling and measurement comparisons difficult. Most consistent and reproducible results are available for the anterior strut chordae. Their normal average length and thickness are reported at ~20mm and 1–2mm respectively (37,39,42,51). Similar to mitral leaflets, chordae adapt to altered loading conditions (42).

4) Papillary muscles

The papillary muscles are labeled by their projected relationship to the mitral commissures as lateral and medial (Figure 1B and 1C) (35). Their bodies originate from the apical 1/3 of the LV and protrude finger-like into the cavity (2). Chordal fans extend from the PM heads to the corresponding anterior, posterior and commissural leaflet portions (Figure 2) (34). The lateral PM in the majority of cases has a single head and dual blood supply from the left

circumflex and left anterior descending artery. The medial PM most commonly has 2 heads and is either supplied by the right or circumflex coronary artery based on dominance (34,35,57). The PM-chordal system is finely tuned so that PM contraction maintains the systolic spatial relationship between the mitral annulus and the PM heads as the intervening myocardium contracts, akin a shock absorber, thereby preventing leaflet prolapse (58–60). The PM head positions and relative distance to each other keep both leaflets under outwardly-directed tension and therefore posteriorly restrained to prevent anterior motion (see hypertrophic 12 cardiomyopathy below). The anterior, posterior and commissural leaflets are therefore in optimal position and configuration to form an effective systolic coaptation seal (61).

2D and 3D Echocardiography of the Mitral Valve Apparatus

Echocardiography is the clinical tool of choice for diagnosing, assessing and following patients with valvular heart disease (62). It is a noninvasive, non-ionizing imaging test with excellent spatial and temporal resolution. Two-dimensional (2D) and threedimensional (3D) Echocardiography (Echo) provides detailed morphologic and functional assessment, while Doppler Echocardiography evaluates hemodynamics. Indeed, the functional mechanisms of mitral regurgitation in many conditions were first clearly defined by Echo. Constant advances in information technology make Echo very portable (63) and an increasingly important tool to guide minimally invasive percutaneous valve repairs (64).

3D Echo has been pivotal to today's understanding of the normal and diseased mitral valve apparatus: 3D Echo established the saddle-shaped, non-planar shape of the mitral annulus (4,6), helped explore the complex geometric relationship of PM and leaflet position relative to the mitral annulus and LV outflow tract (61,65–67) and recently made it possible to measure mitral leaflet size in the beating heart (20,30,42,68). Consequences have been the development of non-planar mitral annuloplasty rings (69), and a detailed understanding of the mechanisms of ischemic/function mitral regurgitation (MR) and systolic anterior motion (SAM) of the anterior leaflet in hypertrophic cardiomyopathy (HCM) (61,65–67), a redefinition of the diagnostic criteria of mitral valve prolapse (MVP) (70,71) and recent evidence of mitral valve adaptation and leaflet growth (30,42,68).

Correct diagnosis of mitral valve disease is dependent on optimally acquired 2D Echo views. A three-dimensional cardiac anatomical understanding is paramount for 2D image acquisition and interpretation. Figure 3 shows the LV and mitral valve in a schematic short-axis view and the Echo beam planes for the most common 2D Echo views. Following the projected 4-Chamber view (4C) Echo beam helps to understand that the mitral valve scallops A3, A2 and P1 are typically shown in this very common Echo view. One can however also appreciate that a slight Echo probe and beam angulation will image a different plane and set of scallops while presenting an apparently similar image (72). 3D Echo controls for such uncertainty since the acquired 3D data can be precisely sliced in every dimension until the optimal and desired 2D view is obtained (73). The middle panel in figure 4 shows a 3D-rendered mitral valve from the surgical perspective (compare with Figure 1C). Slicing the 3D image set perpendicular (red line) to a mediolateral commissural axis (green line) will create 2D Echo views that accurately show the paired leaflet scallops in systole (upper panel) and diastole (lower panel).

Normal and Abnormal Mitral Valve Apparatus Function

Mitral valve anatomy is designed to promote and maintain normal mitral valve apparatus function; perturbations of the normal anatomic relations can result in mitral valve dysfunction (Table 3).

Tightly sealed MV leaflet coaptation depends on the balance of systolic tethering and closing forces on the valve and the amount of leaflet tissue available to cover the mitral annulus (74). Tethering forces are transmitted via the LV wall - PM - chordae system and keep the leaflets from prolapsing into the left atrium (Figure 1A). Closing forces depend on the pressure generated by the LV to close the mitral valve (67,68,75). Disturbance of this finely tuned spatial and temporal interplay of LV contraction, PMs, MV leaflets and mitral annulus can unsettle the tethering force-closing force balance relationship. If this leads to a deficit of leaflet area relative to annulus area coaptation will be impaired and mitral regurgitation occur (67,68,75). A vicious cycle may begin: Significant MR volume will overload the LV; to restore wall tension, the LV will remodel and dilate. Altered LV geometry will consequently remodel the mitral annulus, leaflets and chordae. MR severity will dynamically change throughout these adaptation processes, which conceivably are aimed to restore the tethering force-closing balance relationship (30,42,68). The natural disease course, however, suggests this process is comparable to destructive resonance, with each remodeled component causing disturbance in its relation to all the others. Throughout this, MR severity is a moving target, which, if progressive, will fuel ongoing LV remodeling.

Mitral Valve Prolapse

MVP is defined as mitral leaflet billowing by more than 2mm above the anterior and posterior horns of the mitral annulus during ventricular systole (Figure 5A) (70,71). MVP is usually diagnosed by echocardiography and is a manifestation of degenerative mitral valve disease. Coaptation geometry is altered due to a combination of leaflet and chordal extensibility, redundancy and elongation; whether superior papillary muscle displacement or traction is cause or effect has yet to be determined (76,77) (Figure 5A, dashed line & arrow). The billowing leaflets may appear diffusely thickened “Barlow’s syndrome” or thin except in flail portions “Fibroelastic deficiency” (39). Severe leaflet prolapse or flail leaflets can result in important MR (Table 3). Repair strategies aim to restore effective leaflet coaptation by reducing leaflet redundancy and mitral annular dimensions, and if needed implanting artificial chordae. Suitable mitral valve leaflet characteristics may also allow leaflet free edge approximation at the site of regurgitation (edge-to-edge technique) by a stitch (Alfieri stitch) (78) or a clip (MitraClip) (79). Repair techniques, pioneered by Alain Carpentier, aim to restore leaflet function while preserving the native valve (80). Mitral valve replacement is not commonly indicated with a skilled surgeon.

Functional/Ischemic Mitral Regurgitation

Functional or ischemic MR is caused by MV leaflet tethering to displaced papillary muscles in the setting of a distorted, remodeled LV (Figure 5B). Pathophysiologic changes of LV form or function that increase the distance between PM heads and mitral annulus interfere with adequate leaflet coaptation (81–84). Key LV changes are LV remodeling with global dilatation and increased LV sphericity (67,85–88), or localized LV remodeling (89). If LV remodeling affects the PM-bearing ventricular walls, apical/posterior/posterolateral and outward PM displacement is likely to develop (89–94) (Figure 5B, arrows). Subsequent tethering restricts systolic closure motion of the MV leaflets. Affected leaflets stay “tied back” in the LV cavity, and this prevents a tightly sealed MV closure (Table 3) (66). Repair strategies aim to restore effective leaflet coaptation by reducing leaflet tethering at the PM and mitral annular ends. Therapeutic PM repositioning targets are LV shape (95–97) and function (revascularization (98–100), gene/cell therapy (101–103), cardiac resynchronization therapy (104,105)), PM approximation (106), chordal cutting (53–55,107), leaflet edge-to-edge approximation technique (78,79), mitral annulus area reduction or valve replacement. Overall, functional/ischemic MR therapy strategies that deal with the

annulus, but not the ventricular tethering are often limited, with recurrent MR(108–111); this can be reduced, for example by chordal cutting (112).

Hypertrophic cardiomyopathy

HCM is an autosomal dominant disease of myocyte disarray and fibrosis, morphologically characterized by significant LV hypertrophy in the absence of chronically elevated afterload or infiltrative diseases (e.g. Cardiac amyloidosis) (Figure 5C double-arrow) (113). HCM also involves the papillary muscles and mitral leaflets: Total mass (2-fold) and number of PM heads are increased (114). The PMs are anteriorly displaced (Figure 5C arrow) and the heads positioned closer to each other (61,115). This increases leaflet slack, and like a sail catching a breeze, the anterior leaflet is at risk of being displaced into the LV outflow tract by blood-flow drag forces (systolic anterior motion, SAM) (61,116–120). If anterior leaflet displacement is severe enough to impair posterior leaflet apposition, mitral regurgitation will occur (Figure 5C red lines) (121). Since PM position is a major culprit, septal reduction therapy does not always eliminate SAM (122). In HCM, the leaflets are also frequently elongated (123,124), contributing to leaflet slack and positioning the coaptation point anteriorly to increase the flow drag forces on the enlarged “sail”. After obstruction begins, LV outflow tract narrowing increases velocity above the valve, propagating SAM through airplane like lift forces (125,126). Because of these mechanisms, repair strategies include papillary muscle repositioning and reducing leaflet redundancy (Table 3).

In summary therefore, the MV is an elegantly constructed, well-balanced mechanism. Normal anatomic relations maintain the leaflets within the LV, preventing prolapse, and maintain them below LV outflow tract flow and taut, preventing SAM. Altered leaflet length and PM position can lead to MVP and obstructive SAM, which are both related to leaflet excess, as shown by their occurrence in the same patient (127,128). Conversely, the PM tethering conducive to normal function becomes maladaptive in ischemic MR when the PMs are displaced. Understanding MV anatomic relationships, appreciated by Echo as well as MRI and CT, is therefore essential to understanding its dysfunction in disease and developing optimal therapies (80).

Acknowledgments

Financial support:

This work is supported in part by grant 07CVD04 of the Leducq Foundation, Paris, France, for the Leducq Transatlantic MITRAL Network, and by National Institutes of Health grants K24 HL67434, R01 HL72265, and HL109506.

References

1. Armstrong EJ, Bischoff J. Heart valve development: endothelial cell signaling and differentiation. *Circ Res.* 2004; 95:459–70. [PubMed: 15345668]
2. Oosthoek PW, Wenink AC, Wisse LJ, Gittenberger-de Groot AC. Development of the papillary muscles of the mitral valve: morphogenetic background of parachute-like asymmetric mitral valves and other mitral valve anomalies. *The Journal of thoracic and cardiovascular surgery.* 1998; 116:36–46. [PubMed: 9671895]
3. Schoen FJ. Evolving concepts of cardiac valve dynamics: the continuum of development, functional structure, pathobiology, and tissue engineering. *Circulation.* 2008; 118:1864–80. [PubMed: 18955677]
4. Levine RA, Handschumacher MD, Sanfilippo AJ, et al. Three-dimensional echocardiographic reconstruction of the mitral valve, with implications for the diagnosis of mitral valve prolapse. *Circulation.* 1989; 80:589–98. [PubMed: 2766511]

5. Kopuz C, Erk K, Baris YS, Onderoglu S, Sinav A. Morphometry of the fibrous ring of the mitral valve. *Annals of anatomy = Anatomischer Anzeiger: official organ of the Anatomische Gesellschaft*. 1995; 177:151–4. [PubMed: 7741275]
6. Levine RA, Triulzi MO, Harrigan P, Weyman AE. The relationship of mitral annular shape to the diagnosis of mitral valve prolapse. *Circulation*. 1987; 75:756–67. [PubMed: 3829339]
7. Puff, A. *Ischemic Mitral Incompetence*. New York: Springer; 1991.
8. Timek TA, Green GR, Tibayan FA, et al. Aorto-mitral annular dynamics. *The Annals of thoracic surgery*. 2003; 76:1944–50. [PubMed: 14667619]
9. Lansac E, Lim KH, Shomura Y, et al. Dynamic balance of the aortomitral junction. *The Journal of thoracic and cardiovascular surgery*. 2002; 123:911–8. [PubMed: 12019376]
10. Veronesi F, Corsi C, Sugeng L, et al. Quantification of mitral apparatus dynamics in functional and ischemic mitral regurgitation using real-time 3-dimensional echocardiography. *Journal of the American Society of Echocardiography: official publication of the American Society of Echocardiography*. 2008; 21:347–54. [PubMed: 17681731]
11. Hamdan A, Guetta V, Konen E, et al. Deformation dynamics and mechanical properties of the aortic annulus by 4-dimensional computed tomography: insights into the functional anatomy of the aortic valve complex and implications for transcatheter aortic valve therapy. *Journal of the American College of Cardiology*. 2012; 59:119–27. [PubMed: 22222074]
12. Komoda T, Hetzer R, Oellinger J, et al. Mitral annular flexibility. *Journal of cardiac surgery*. 1997; 12:102–9. [PubMed: 9271730]
13. Salgo IS, Gorman JH 3rd, Gorman RC, et al. Effect of annular shape on leaflet curvature in reducing mitral leaflet stress. *Circulation*. 2002; 106:711–7. [PubMed: 12163432]
14. Kunzelman KS, Reimink MS, Cochran RP. Annular dilatation increases stress in the mitral valve and delays coaptation: a finite element computer model. *Cardiovascular surgery (London, England)*. 1997; 5:427–34.
15. Jimenez JH, Liou SW, Padala M, et al. A saddle-shaped annulus reduces systolic strain on the central region of the mitral valve anterior leaflet. *The Journal of thoracic and cardiovascular surgery*. 2007; 134:1562–8. [PubMed: 18023684]
16. Padala M, Hutchison RA, Croft LR, et al. Saddle shape of the mitral annulus reduces systolic strains on the P2 segment of the posterior mitral leaflet. *The Annals of thoracic surgery*. 2009; 88:1499–504. [PubMed: 19853100]
17. Reimink MS, Kunzelman KS, Verrier ED, Cochran RP. The effect of anterior chordal replacement on mitral valve function and stresses. A finite element study. *ASAIO journal (American Society for Artificial Internal Organs)*. 1995; 41:M754–62. [PubMed: 8573908]
18. Jensen MO, Jensen H, Smerup M, et al. Saddle-shaped mitral valve annuloplasty rings experience lower forces compared with flat rings. *Circulation*. 2008; 118:S250–5. [PubMed: 18824763]
19. Jensen MO, Jensen H, Levine RA, et al. Saddle-shaped mitral valve annuloplasty rings improve leaflet coaptation geometry. *The Journal of thoracic and cardiovascular surgery*. 2011; 142:697–703. [PubMed: 21329946]
20. Jensen MO, Hagege AA, Otsuji Y, Levine RA. The unsaddled annulus: biomechanical culprit in mitral valve prolapse? *Circulation*. 2013; 127:766–8. [PubMed: 23429895]
21. T, Tamura K, Tanaka S, Asano G. Blood vessels in normal and abnormal mitral valve leaflets. *Journal of Nippon Medical School = Nippon Ika Daigaku zasshi*. 2001; 68:171–80. [PubMed: 11301363]
22. Williams TH, Folan JC, Jew JY, Wang YF. Variations in atrioventricular valve innervation in four species of mammals. *The American journal of anatomy*. 1990; 187:193–200. [PubMed: 2301279]
23. Swanson JC, Davis LR, Arata K, et al. Characterization of mitral valve anterior leaflet perfusion patterns. *The Journal of heart valve disease*. 2009; 18:488–95. [PubMed: 20099688]
24. Carceller-Blanchard AM, Fouron JC. Determinants of the Doppler flow velocity profile through the mitral valve of the human fetus. *British heart journal*. 1993; 70:457–60. [PubMed: 8260278]
25. Maffessanti F, Gripari P, Pontone G, et al. Three-dimensional dynamic assessment of tricuspid and mitral annuli using cardiovascular magnetic resonance. *European heart journal cardiovascular Imaging*. 2013

26. Veronesi F, Corsi C, Sugeng L, et al. A study of functional anatomy of aorticmitral valve coupling using 3D matrix transesophageal echocardiography. *Circulation Cardiovascular imaging*. 2009; 2:24–31. [PubMed: 19808561]
27. Alkadhhi H, Desbiolles L, Stolzmann P, et al. Mitral annular shape, size, and motion in normals and in patients with cardiomyopathy: evaluation with computed tomography. *Investigative radiology*. 2009; 44:218–25. [PubMed: 19212270]
28. Ormiston JA, Shah PM, Tei C, Wong M. Size and motion of the mitral valve annulus in man. I. A two-dimensional echocardiographic method and findings in normal subjects. *Circulation*. 1981; 64:113–20. [PubMed: 7237707]
29. Flachskampf FA, Chandra S, Gaddipatti A, et al. Analysis of shape and motion of the mitral annulus in subjects with and without cardiomyopathy by echocardiographic 3-dimensional reconstruction. *Journal of the American Society of Echocardiography: official publication of the American Society of Echocardiography*. 2000; 13:277–87. [PubMed: 10756245]
30. Chaput M, Handschumacher MD, Tournoux F, et al. Mitral leaflet adaptation to ventricular remodeling: occurrence and adequacy in patients with functional mitral regurgitation. *Circulation*. 2008; 118:845–52. [PubMed: 18678770]
31. Watanabe N, Ogasawara Y, Yamaura Y, et al. Mitral annulus flattens in ischemic mitral regurgitation: geometric differences between inferior and anterior myocardial infarction: a real-time 3-dimensional echocardiographic study. *Circulation*. 2005; 112:1458–62. [PubMed: 16159863]
32. Daimon M, Saracino G, Fukuda S, et al. Dynamic change of mitral annular geometry and motion in ischemic mitral regurgitation assessed by a computerized 3D echo method. *Echocardiography (Mount Kisco, NY)*. 2010; 27:1069–77.
33. Lee AP, Hsiung MC, Salgo IS, et al. Quantitative analysis of mitral valve morphology in mitral valve prolapse with real-time 3-dimensional echocardiography: importance of annular saddle shape in the pathogenesis of mitral regurgitation. *Circulation*. 2013; 127:832–41. [PubMed: 23266859]
34. Chiechi MA, Lees WM, Thompson R. Functional anatomy of the normal mitral valve. *The Journal of thoracic surgery*. 1956; 32:378–98. [PubMed: 13358125]
35. Rusted IE, Scheifley CH, Edwards JE. Studies of the mitral valve. I. Anatomic features of the normal mitral valve and associated structures. *Circulation*. 1952; 6:825–31. [PubMed: 12998105]
36. Fenoglio JJ Jr, Tuan Duc P, Wit AL, Bassett AL, Wagner BM. Canine mitral complex. Ultrastructure and electromechanical properties. *Circulation research*. 1972; 31:417–30. [PubMed: 5057021]
37. Lam JH, Ranganathan N, Wigle ED, Silver MD. Morphology of the human mitral valve. I. Chordae tendineae: a new classification. *Circulation*. 1970; 41:449–58. [PubMed: 5415982]
38. Cochran RP, Kunzelman KS, Chuong CJ, Sacks MS, Eberhart RC. Nondestructive analysis of mitral valve collagen fiber orientation. *ASAIO transactions/American Society for Artificial Internal Organs*. 1991; 37:M447–8. [PubMed: 1751231]
39. Carpentier, A.; Guerinon, J.; Deloche, A.; Fabiani, JN.; Relland, M. *THE MITRAL VALVE-A Pluridisciplinary Approach*. Acton, MA: Publishing Sciences Group Inc; 1976.
40. Laniado S, Yellin EL, Miller H, Frater RW. Temporal relation of the first heart sound to closure of the mitral valve. *Circulation*. 1973; 47:1006–14. [PubMed: 4705568]
41. Nkomo VT, Gardin JM, Skelton TN, Gottdiener JS, Scott CG, Enriquez-Sarano M. Burden of valvular heart diseases: a population-based study. *Lancet*. 2006; 368:1005–11. [PubMed: 16980116]
42. Dal-Bianco JP, Aikawa E, Bischoff J, et al. Active adaptation of the tethered mitral valve: insights into a compensatory mechanism for functional mitral regurgitation. *Circulation*. 2009; 120:334–42. [PubMed: 19597052]
43. Kunzelman KS, Cochran RP, Chuong C, Ring WS, Verrier ED, Eberhart RD. Finite element analysis of the mitral valve. *The Journal of heart valve disease*. 1993; 2:326–40. [PubMed: 8269128]

44. Kunzelman KS, Cochran RP, Murphree SS, Ring WS, Verrier ED, Eberhart RC. Differential collagen distribution in the mitral valve and its influence on biomechanical behaviour. *The Journal of heart valve disease*. 1993; 2:236–44. [PubMed: 8261162]
45. Marron K, Yacoub MH, Polak JM, et al. Innervation of human atrioventricular and arterial valves. *Circulation*. 1996; 94:368–75. [PubMed: 8759078]
46. Jew JY, Williams TH. Innervation of the mitral valve is strikingly depleted with age. *The Anatomical record*. 1999; 255:252–60. [PubMed: 10411393]
47. Noguchi T, Shimada T, Nakamura M, Uchida Y, Shirabe J. The distribution and structure of the lymphatic system in dog atrioventricular valves. *Archives of histology and cytology*. 1988; 51:361–70. [PubMed: 3147693]
48. Aikawa E, Whittaker P, Farber M, et al. Human semilunar cardiac valve remodeling by activated cells from fetus to adult: implications for postnatal adaptation, pathology, and tissue engineering. *Circulation*. 2006; 113:1344–52. [PubMed: 16534030]
49. Quick DW, Kunzelman KS, Kneebone JM, Cochran RP. Collagen synthesis is upregulated in mitral valves subjected to altered stress. *ASAIO journal (American Society for Artificial Internal Organs)*. 1997; 43:181–6. [PubMed: 9152488]
50. Millington-Sanders C, Meir A, Lawrence L, Stolinski C. Structure of chordae tendineae in the left ventricle of the human heart. *Journal of anatomy*. 1998; 192 (Pt 4):573–81. [PubMed: 9723984]
51. Degandt AA, Weber PA, Saber HA, Duran CM. Mitral valve basal chordae: comparative anatomy and terminology. *The Annals of thoracic surgery*. 2007; 84:1250–5. [PubMed: 17888977]
52. Liao J, Vesely I. A structural basis for the size-related mechanical properties of mitral valve chordae tendineae. *Journal of biomechanics*. 2003; 36:1125–33. [PubMed: 12831738]
53. Messas E, Guerrero JL, Handschumacher MD, et al. Chordal cutting: a new therapeutic approach for ischemic mitral regurgitation. *Circulation*. 2001; 104:1958–63. [PubMed: 11602501]
54. Messas E, Pouzet B, Touchot B, et al. Efficacy of chordal cutting to relieve chronic persistent ischemic mitral regurgitation. *Circulation*. 2003; 108(Suppl 1):II111–5. [PubMed: 12970218]
55. Messas E, Yosefy C, Chaput M, et al. Chordal cutting does not adversely affect left ventricle contractile function. *Circulation*. 2006; 114:1524–8. [PubMed: 16820631]
56. Obadia JF, Casali C, Chassignolle JF, Janier M. Mitral subvalvular apparatus: different functions of primary and secondary chordae. *Circulation*. 1997; 96:3124–8. [PubMed: 9386184]
57. Victor S, Nayak VM. Variations in the papillary muscles of the normal mitral valve and their surgical relevance. *Journal of cardiac surgery*. 1995; 10:597–607. [PubMed: 7488788]
58. Komeda M, Glasson JR, Bolger AF, Daughters GT 2nd, Ingels NB Jr, Miller DC. Papillary muscle-left ventricular wall “complex”. *The Journal of thoracic and cardiovascular surgery*. 1997; 113:292–300. discussion 300–1. [PubMed: 9040623]
59. Joudinaud TM, Kegel CL, Flecher EM, et al. The papillary muscles as shock absorbers of the mitral valve complex. An experimental study *European journal of cardio-thoracic surgery: official journal of the European Association for Cardio-thoracic Surgery*. 2007; 32:96–101.
60. Gorman JH 3rd, Gupta KB, Streicher JT, et al. Dynamic three-dimensional imaging of the mitral valve and left ventricle by rapid sonomicrometry array localization. *The Journal of thoracic and cardiovascular surgery*. 1996; 112:712–26. [PubMed: 8800160]
61. Jiang L, Levine RA, King ME, Weyman AE. An integrated mechanism for systolic anterior motion of the mitral valve in hypertrophic cardiomyopathy based on echocardiographic observations. *Am Heart J*. 1987; 113:633–44. [PubMed: 3825854]
62. Bonow RO, Carabello BA, Kanu C, et al. ACC/AHA 2006 guidelines for the management of patients with valvular heart disease: a report of the American College of Cardiology/American Heart Association Task Force on Practice Guidelines (writing committee to revise the 1998 Guidelines for the Management of Patients With Valvular Heart Disease): developed in collaboration with the Society of Cardiovascular Anesthesiologists: endorsed by the Society for Cardiovascular Angiography and Interventions and the Society of Thoracic Surgeons. *Circulation*. 2006; 114:e84–231. [PubMed: 16880336]
63. Weiner RB, Wang F, Hutter AM Jr, et al. The feasibility, diagnostic yield, and learning curve of portable echocardiography for out-of-hospital cardiovascular disease screening. *Journal of the*

- American Society of Echocardiography: official publication of the American Society of Echocardiography. 2012; 25:568–75. [PubMed: 22326132]
64. Zamorano JL, Badano LP, Bruce C, et al. EAE/ASE recommendations for the use of echocardiography in new transcatheter interventions for valvular heart disease. *European heart journal*. 2011; 32:2189–214. [PubMed: 21885465]
 65. Messas E, Guerrero JL, Handschumacher MD, et al. Paradoxical decrease in ischemic mitral regurgitation with papillary muscle dysfunction: insights from three-dimensional and contrast echocardiography with strain rate measurement. *Circulation*. 2001; 104:1952–7. [PubMed: 11602500]
 66. Otsuji Y, Gilon D, Jiang L, et al. Restricted diastolic opening of the mitral leaflets in patients with left ventricular dysfunction: evidence for increased valve tethering. *J Am Coll Cardiol*. 1998; 32:398–404. [PubMed: 9708467]
 67. Otsuji Y, Handschumacher MD, Schwammenthal E, et al. Insights from threedimensional echocardiography into the mechanism of functional mitral regurgitation: direct in vivo demonstration of altered leaflet tethering geometry. *Circulation*. 1997; 96:1999–2008. [PubMed: 9323092]
 68. Chaput M, Handschumacher MD, Guerrero JL, et al. Mitral leaflet adaptation to ventricular remodeling: prospective changes in a model of ischemic mitral regurgitation. *Circulation*. 2009; 120:S99–103. [PubMed: 19752393]
 69. Carpentier AF, Lessana A, Relland JY, et al. The “physio-ring”: an advanced concept in mitral valve annuloplasty. *The Annals of thoracic surgery*. 1995; 60:1177–85. discussion 1185–6. [PubMed: 8526596]
 70. Levine RA, Stathogiannis E, Newell JB, Harrigan P, Weyman AE. Reconsideration of echocardiographic standards for mitral valve prolapse: lack of association between leaflet displacement isolated to the apical four chamber view and independent echocardiographic evidence of abnormality. *Journal of the American College of Cardiology*. 1988; 11:1010–9. [PubMed: 3281989]
 71. Freed LA, Levy D, Levine RA, et al. Prevalence and clinical outcome of mitralvalve prolapse. *The New England journal of medicine*. 1999; 341:1–7. [PubMed: 10387935]
 72. King DL, Harrison MR, King DL Jr, Gopal AS, Kwan OL, DeMaria AN. Ultrasound beam orientation during standard two-dimensional imaging: assessment by three-dimensional echocardiography. *Journal of the American Society of Echocardiography: official publication of the American Society of Echocardiography*. 1992; 5:569–76. [PubMed: 1466881]
 73. Lang RM, Badano LP, Tsang W, et al. EAE/ASE recommendations for image acquisition and display using three-dimensional echocardiography. *European heart journal cardiovascular Imaging*. 2012; 13:1–46. [PubMed: 22275509]
 74. Levy MJ, Edwards JE. Anatomy of mitral insufficiency. *Progress in cardiovascular diseases*. 1962; 5:119–44. [PubMed: 14464797]
 75. Levine RA, Schwammenthal E. Ischemic mitral regurgitation on the threshold of a solution: from paradoxes to unifying concepts. *Circulation*. 2005; 112:745–58. [PubMed: 16061756]
 76. Sanfilippo AJ, Harrigan P, Popovic AD, Weyman AE, Levine RA. Papillary muscle traction in mitral valve prolapse: quantitation by two-dimensional echocardiography. *Journal of the American College of Cardiology*. 1992; 19:564–71. [PubMed: 1538011]
 77. Gornick CC, Tobler HG, Pritzker MC, Tuna IC, Almquist A, Benditt DG. Electrophysiologic effects of papillary muscle traction in the intact heart. *Circulation*. 1986; 73:1013–21. [PubMed: 3698223]
 78. Fucci C, Sandrelli L, Pardini A, Torracca L, Ferrari M, Alfieri O. Improved results with mitral valve repair using new surgical techniques. *European journal of cardio-thoracic surgery: official journal of the European Association for Cardiothoracic Surgery*. 1995; 9:621–6. discuss 626–7.
 79. Feldman T, Kar S, Rinaldi M, et al. Percutaneous mitral repair with the MitraClip system: safety and midterm durability in the initial EVEREST (Endovascular Valve Edge-to-Edge REpair Study) cohort. *Journal of the American College of Cardiology*. 2009; 54:686–94. [PubMed: 19679246]
 80. Carpentier A. Cardiac valve surgery--the “French correction”. *The Journal of thoracic and cardiovascular surgery*. 1983; 86:323–37. [PubMed: 6887954]

81. Perloff JK, Roberts WC. The mitral apparatus. Functional anatomy of mitral regurgitation. *Circulation*. 1972; 46:227–39.
82. Silverman ME, Hurst JW. The mitral complex. Interaction of the anatomy, physiology, and pathology of the mitral annulus, mitral valve leaflets, chordae tendineae, and papillary muscles. *Am Heart J*. 1968; 76:399–418. [PubMed: 4952735]
83. Godley RW, Wann LS, Rogers EW, Feigenbaum H, Weyman AE. Incomplete mitral leaflet closure in patients with papillary muscle dysfunction. *Circulation*. 1981; 63:565–71. [PubMed: 7460242]
84. Ogawa S, Hubbard FE, Mardelli TJ, Dreifus LS. Cross-sectional echocardiographic spectrum of papillary muscle dysfunction. *Am Heart J*. 1979; 97:312–21. [PubMed: 420070]
85. Kaul S, Spotnitz WD, Glasheen WP, Touchstone DA. Mechanism of ischemic mitral regurgitation. An experimental evaluation. *Circulation*. 1991; 84:2167–80. [PubMed: 1934385]
86. Kono T, Sabbah HN, Rosman H, Alam M, Jafri S, Goldstein S. Left ventricular shape is the primary determinant of functional mitral regurgitation in heart failure. *J Am Coll Cardiol*. 1992; 20:1594–8. [PubMed: 1452934]
87. Sabbah HN, Kono T, Stein PD, Mancini GB, Goldstein S. Left ventricular shape changes during the course of evolving heart failure. *Am J Physiol*. 1992; 263:H266–70. [PubMed: 1636764]
88. Sabbah HN, Rosman H, Kono T, Alam M, Khaja F, Goldstein S. On the mechanism of functional mitral regurgitation. *Am J Cardiol*. 1993; 72:1074–6. [PubMed: 8213590]
89. Yiu SF, Enriquez-Sarano M, Tribouilloy C, Seward JB, Tajik AJ. Determinants of the degree of functional mitral regurgitation in patients with systolic left ventricular dysfunction: A quantitative clinical study. *Circulation*. 2000; 102:1400–6. [PubMed: 10993859]
90. Otsuji Y, Handschumacher MD, Liel-Cohen N, et al. Mechanism of ischemic mitral regurgitation with segmental left ventricular dysfunction: three-dimensional echocardiographic studies in models of acute and chronic progressive regurgitation. *J Am Coll Cardiol*. 2001; 37:641–8. [PubMed: 11216991]
91. He S, Fontaine AA, Schwammenthal E, Yoganathan AP, Levine RA. Integrated mechanism for functional mitral regurgitation: leaflet restriction versus coapting force: in vitro studies. *Circulation*. 1997; 96:1826–34. [PubMed: 9323068]
92. Gorman RC, McCaughan JS, Ratcliffe MB, et al. Pathogenesis of acute ischemic mitral regurgitation in three dimensions. *J Thorac Cardiovasc Surg*. 1995; 109:684–93. [PubMed: 7715215]
93. Liel-Cohen N, Guerrero JL, Otsuji Y, et al. Design of a new surgical approach for ventricular remodeling to relieve ischemic mitral regurgitation: insights from 3- dimensional echocardiography. *Circulation*. 2000; 101:2756–63. [PubMed: 10851215]
94. Llaneras MR, Nance ML, Streicher JT, et al. Large animal model of ischemic mitral regurgitation. *Ann Thorac Surg*. 1994; 57:432–9. [PubMed: 8311608]
95. Hung J, Chaput M, Guerrero JL, et al. Persistent reduction of ischemic mitral regurgitation by papillary muscle repositioning: structural stabilization of the papillary muscle-ventricular wall complex. *Circulation*. 2007; 116:I259–63. [PubMed: 17846314]
96. Hung J, Guerrero JL, Handschumacher MD, Supple G, Sullivan S, Levine RA. Reverse ventricular remodeling reduces ischemic mitral regurgitation: echoguided device application in the beating heart. *Circulation*. 2002; 106:2594–600. [PubMed: 12427657]
97. Solis J, Levine RA, Johnson B, et al. Polymer injection therapy to reverse remodel the papillary muscles: efficacy in reducing mitral regurgitation in a chronic ischemic model. *Circulation Cardiovascular interventions*. 2010; 3:499–505. [PubMed: 20736444]
98. Di Donato M, Frigiola A, Menicanti L, et al. Moderate ischemic mitral regurgitation and coronary artery bypass surgery: effect of mitral repair on clinical outcome. *J Heart Valve Dis*. 2003; 12:272–9. [PubMed: 12803324]
99. Trichon BH, Glower DD, Shaw LK, et al. Survival after coronary revascularization, with and without mitral valve surgery, in patients with ischemic mitral regurgitation. *Circulation*. 2003; 108(Suppl 1):II103–10. [PubMed: 12970217]
100. Tenenbaum A, Leor J, Motro M, et al. Improved posterobasal segment function after thrombolysis is associated with decreased incidence of significant mitral regurgitation in a first

- inferior myocardial infarction. *Journal of the American College of Cardiology*. 1995; 25:1558–63. [PubMed: 7759707]
101. Beeri R, Guerrero JL, Supple G, Sullivan S, Levine RA, Hajjar RJ. New efficient catheter-based system for myocardial gene delivery. *Circulation*. 2002; 106:1756–9. [PubMed: 12356625]
 102. Cittadini A, Monti MG, Iaccarino G, et al. Adenoviral gene transfer of Akt enhances myocardial contractility and intracellular calcium handling. *Gene Ther*. 2006; 13:8–19. [PubMed: 16094411]
 103. Hagege AA, Marolleau JP, Vilquin JT, et al. Skeletal myoblast transplantation in ischemic heart failure: long-term follow-up of the first phase I cohort of patients. *Circulation*. 2006; 114:1108–13. [PubMed: 16820558]
 104. Kanzaki H, Bazaz R, Schwartzman D, Dohi K, Sade LE, Gorcsan J 3rd. A mechanism for immediate reduction in mitral regurgitation after cardiac resynchronization therapy: insights from mechanical activation strain mapping. *Journal of the American College of Cardiology*. 2004; 44:1619–25. [PubMed: 15489094]
 105. Solis J, McCarty D, Levine RA, et al. Mechanism of decrease in mitral regurgitation after cardiac resynchronization therapy: optimization of the forcebalance relationship. *Circulation Cardiovascular imaging*. 2009; 2:444–50. [PubMed: 19920042]
 106. Matsui Y, Suto Y, Shimura S, et al. Impact of papillary muscles approximation on the adequacy of mitral coaptation in functional mitral regurgitation due to dilated cardiomyopathy. *Annals of thoracic and cardiovascular surgery: official journal of the Association of Thoracic and Cardiovascular Surgeons of Asia*. 2005; 11:164–71. [PubMed: 16030475]
 107. Messas E, Bel A, Szymanski C, et al. Relief of Mitral Leaflet Tethering Following Chronic Myocardial Infarction by Chordal Cutting Diminishes Left Ventricular Remodeling. *Circ Cardiovasc Imaging* 2010. 2010 Sep 8. [Epub ahead of print].
 108. Hung J, Papakostas L, Tahta SA, et al. Mechanism of recurrent ischemic mitral regurgitation after annuloplasty: continued LV remodeling as a moving target. *Circulation*. 2004; 110:II85–90. [PubMed: 15364844]
 109. Kuwahara E, Otsuji Y, Iguro Y, et al. Mechanism of recurrent/persistent ischemic/functional mitral regurgitation in the chronic phase after surgical annuloplasty: importance of augmented posterior leaflet tethering. *Circulation*. 2006; 114:I529–34. [PubMed: 16820632]
 110. Liel-Cohen N, Otsuji Y, Vlahakes G, Akins C, Levine R. Functional Ischemic Mitral Regurgitation Can Persist Despite Ring Annuloplasty: Mechanistic Insights. *Circulation*. 1997; 96:I-540.
 111. McGee EC, Gillinov AM, Blackstone EH, et al. Recurrent mitral regurgitation after annuloplasty for functional ischemic mitral regurgitation. *The Journal of thoracic and cardiovascular surgery*. 2004; 128:916–24. [PubMed: 15573077]
 112. Borger MA, Murphy PM, Alam A, et al. Initial results of the chordal-cutting operation for ischemic mitral regurgitation. *The Journal of thoracic and cardiovascular surgery*. 2007; 133:1483–92. [PubMed: 17532944]
 113. Watkins H, Ashrafian H, Redwood C. Inherited cardiomyopathies. *The New England journal of medicine*. 2011; 364:1643–56. [PubMed: 21524215]
 114. Harrigan CJ, Appelbaum E, Maron BJ, et al. Significance of papillary muscle abnormalities identified by cardiovascular magnetic resonance in hypertrophic cardiomyopathy. *The American journal of cardiology*. 2008; 101:668–73. [PubMed: 18308018]
 115. Hwang HJ, Choi EY, Kwan J, et al. Dynamic change of mitral apparatus as potential cause of left ventricular outflow tract obstruction in hypertrophic cardiomyopathy. *European journal of echocardiography: the journal of the Working Group on Echocardiography of the European Society of Cardiology*. 2011; 12:19–25. [PubMed: 20693545]
 116. Levine RA, Vlahakes GJ, Lefebvre X, et al. Papillary muscle displacement causes systolic anterior motion of the mitral valve. Experimental validation and insights into the mechanism of subaortic obstruction. *Circulation*. 1995; 91:1189–95. [PubMed: 7850958]
 117. Sherrid MV, Chu CK, Delia E, Mogtader A, Dwyer EM Jr. An echocardiographic study of the fluid mechanics of obstruction in hypertrophic cardiomyopathy. *Journal of the American College of Cardiology*. 1993; 22:816–25. [PubMed: 8354817]

118. Sherrid MV, Gunsburg DZ, Moldenhauer S, Pearle G. Systolic anterior motion begins at low left ventricular outflow tract velocity in obstructive hypertrophic cardiomyopathy. *Journal of the American College of Cardiology*. 2000; 36:1344–54. [PubMed: 11028493]
119. Maron BJ, Gottdiener JS, Roberts WC, Henry WL, Savage DD, Epstein SE. Left ventricular outflow tract obstruction due to systolic anterior motion of the anterior mitral leaflet in patients with concentric left ventricular hypertrophy. *Circulation*. 1978; 57:527–33. [PubMed: 564246]
120. Maron BJ, Epstein SE. Hypertrophic cardiomyopathy. Recent observations regarding the specificity of three hallmarks of the disease: asymmetric septal hypertrophy, septal disorganization and systolic anterior motion of the anterior mitral leaflet. *The American journal of cardiology*. 1980; 45:141–54. [PubMed: 6985764]
121. Schwammenthal E, Nakatani S, He S, et al. Mechanism of mitral regurgitation in hypertrophic cardiomyopathy: mismatch of posterior to anterior leaflet length and mobility. *Circulation*. 1998; 98:856–65. [PubMed: 9738640]
122. Delling FN, Sanborn DY, Levine RA, et al. Frequency and mechanism of persistent systolic anterior motion and mitral regurgitation after septal ablation in obstructive hypertrophic cardiomyopathy. *The American journal of cardiology*. 2007; 100:1691–5. [PubMed: 18036370]
123. Klues HG, Roberts WC, Maron BJ. Morphological determinants of echocardiographic patterns of mitral valve systolic anterior motion in obstructive hypertrophic cardiomyopathy. *Circulation*. 1993; 87:1570–9. [PubMed: 8491013]
124. Kim DH, Handschumacher MD, Levine RA, et al. In vivo measurement of mitral leaflet surface area and subvalvular geometry in patients with asymmetrical septal hypertrophy: insights into the mechanism of outflow tract obstruction. *Circulation*. 2010; 122:1298–307. [PubMed: 20837895]
125. Hagege AA, Bruneval P, Levine RA, Desnos M, Neamatalla H, Judge DP. The mitral valve in hypertrophic cardiomyopathy: old versus new concepts. *Journal of cardiovascular translational research*. 2011; 4:757–66. [PubMed: 21909825]
126. He S, Hopmeyer J, Lefebvre XP, Schwammenthal E, Yoganathan AP, Levine RA. Importance of leaflet elongation in causing systolic anterior motion of the mitral valve. *The Journal of heart valve disease*. 1997; 6:149–59. [PubMed: 9130123]
127. Maslow AD, Regan MM, Haering JM, Johnson RG, Levine RA. Echocardiographic predictors of left ventricular outflow tract obstruction and systolic anterior motion of the mitral valve after mitral valve reconstruction for myxomatous valve disease. *Journal of the American College of Cardiology*. 1999; 34:2096–104. [PubMed: 10588230]
128. Jebara VA, Mihaileanu S, Acar C, et al. Left ventricular outflow tract obstruction after mitral valve repair. Results of the sliding leaflet technique. *Circulation*. 1993; 88:II30–4. [PubMed: 8222170]
129. Bulkley BH, Roberts WC. Dilatation of the mitral annulus. A rare cause of mitral regurgitation. *The American journal of medicine*. 1975; 59:457–63. [PubMed: 1172652]
130. Komoda T, Hetzer R, Uyama C, et al. Mitral annular function assessed by 3D imaging for mitral valve surgery. *The Journal of heart valve disease*. 1994; 3:483–90. [PubMed: 8000581]
131. Mautner SL, Klues HG, Mautner GC, Proschan MA, Roberts WC, Maron BJ. Comparison of mitral valve dimensions in adults with valvular aortic stenosis, pure aortic regurgitation and hypertrophic cardiomyopathy. *The American journal of cardiology*. 1993; 71:949–53. [PubMed: 8465787]
132. Klues HG, Maron BJ, Dollar AL, Roberts WC. Diversity of structural mitral valve alterations in hypertrophic cardiomyopathy. *Circulation*. 1992; 85:1651–60. [PubMed: 1572023]

Keypoints

- The mitral valve apparatus is a complex three-dimensional functional unit that is critical to unidirectional heart pump function.
- The main mitral valve apparatus components are 1) mitral annulus, 2) mitral valve leaflets, 3) chordae tendineae and 4) papillary muscles.
- Tight sealed mitral leaflet coaptation depends on the balance of systolic tethering and closing forces on the valve and on the amount of leaflet tissue available.
- Echocardiography is ideally suited to examine the mitral valve apparatus and has provided insights into the mechanism of mitral valve disease.
- Understanding normal mitral valve apparatus function is essential to comprehend alterations in mitral valve disease and the rationale for repair strategies.

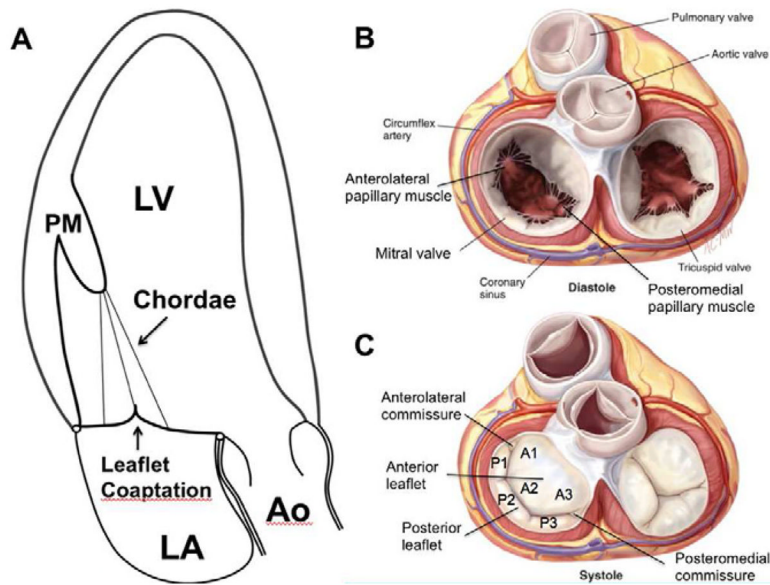


Figure 1.

A. Schematic apical long-axis view of the heart in systole with the apex on top. There is normal function and spatial relationship of the left ventricular myocardium, the papillary muscles (PM), chordae, leaflets and mitral annulus. The tethering force closing force balance relationship is normal, both leaflets are normally configured, concave toward the LV, and coapt without mitral regurgitation. B. Surgical view of the open mitral valve in diastole with the atrial walls removed. C. Surgical view of the closed mitral valve in systole. (Ao, aorta; LA, left atrium; LV, left ventricle; PM, papillary muscle; Panels B and C are adapted from Carpentier A et al. Carpentier's Reconstructive Valve Surgery. From Valve Analysis to Valve Reconstruction. 2010 Saunders Elsevier)

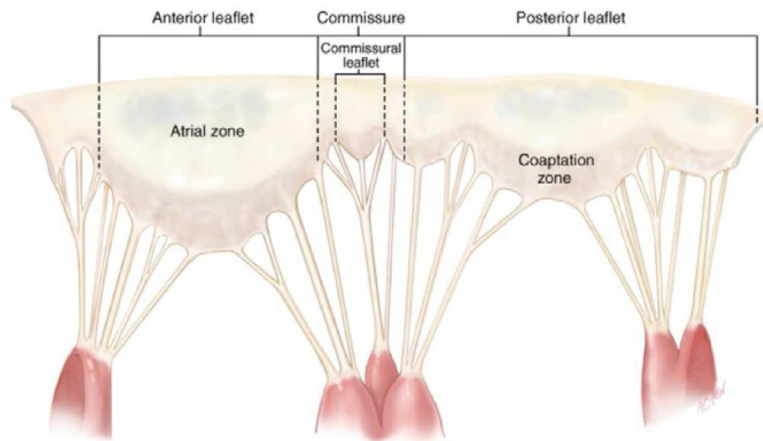


Figure 2. The mitral valve is unfolded and the atrial leaflet surface exposed. The papillary muscles have been dissected and the heads remain attached via chordae tendineae to the anterior, posterior and commissural leaflets (Adapted from Carpentier A et al. Carpentier's Reconstructive Valve Surgery. From Valve Analysis to Valve Reconstruction. 2010 Saunders Elsevier)

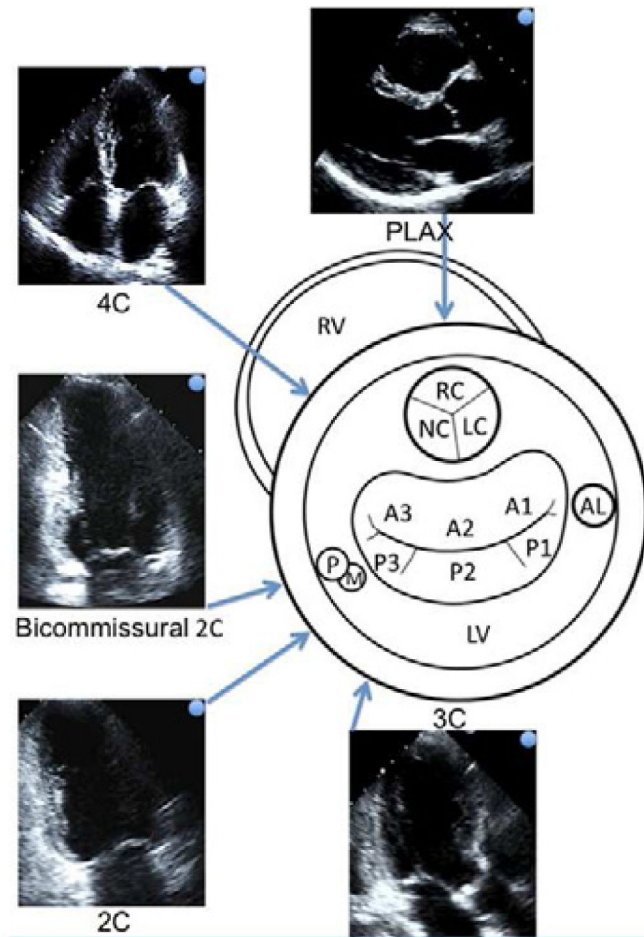


Figure 3.

The central schematic shows the left ventricle in short axis view seen from the apex. The approximate locations of the aortic valve, mitral valve and papillary muscles are projected. The most common and standardized 2D Echo views are arranged around the schematic. The blue arrow-tipped lines indicate the direction of the Echo beam and are connected to the corresponding Echo views. The blue dots on the Echo images relate to the orientation of the blue arrows. Extrapolating the Echo beam lines allows us to estimate the 2D Echo mitral scallops represented in the corresponding Echo views. (2C, 2-Chamber view; 4C, 4-Chamber view; AL, anterolateral papillary muscle; LC, left aortic cusp; LV, left ventricle; NC, noncoronary aortic cusp; PLAX, parasternal long axis view; RC, right coronary cusp; RV, right ventricle; PM, posterolateral papillary muscle).

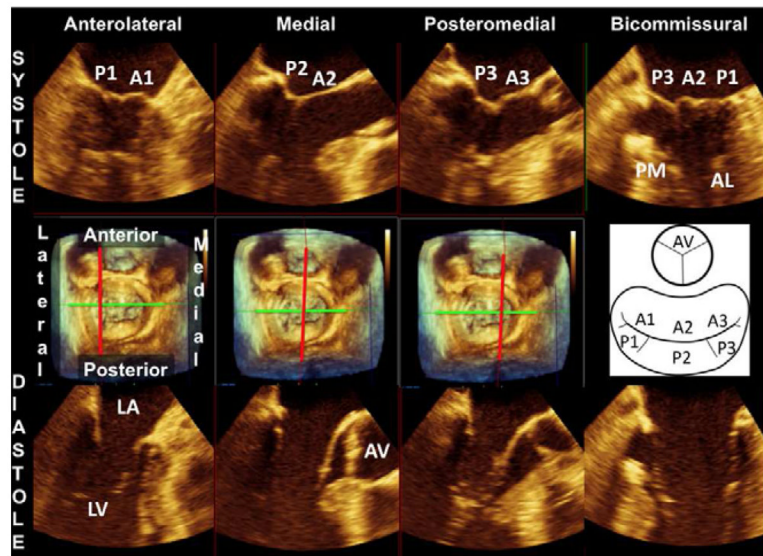


Figure 4.

The middle panel shows a 3D-rendered surgical view of the mitral valve. A schematic on the right side of the middle panel helps identify the mitral valve scallops and aortic valve in this view. The upper panel shows 2D Echo views of precisely known orientation because they are derived as slices of the 3D mitral valve apparatus in systole. The slice plane is indicated by the red line in the middle plane (perpendicular to a bicommissural axis, green line). The lower panel shows the same slice planes in diastole with the mitral leaflets open. (AL, anterolateral papillary muscle; AV, aortic valve; LA, left atrium; LV, left ventricle; PM, posteromedial papillary muscle)

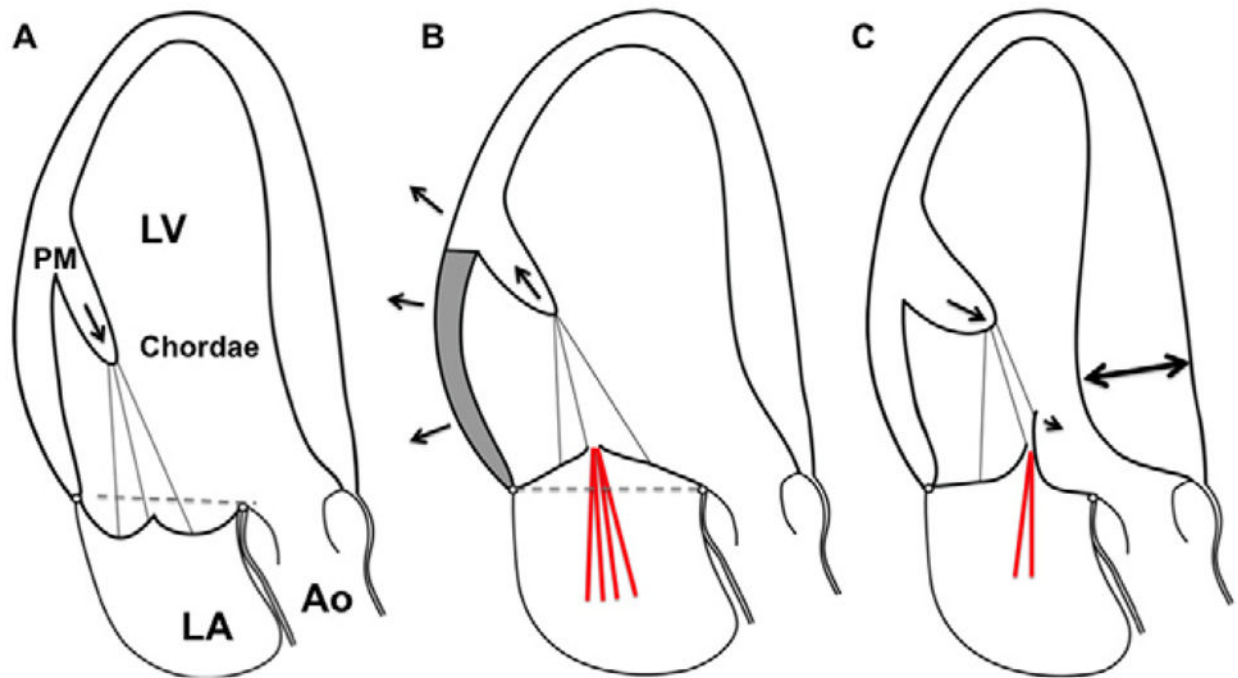


Figure 5.

A. Mitral valve prolapse: The schematic shows bileaflet mitral valve prolapse, with superior displacement of the papillary muscle tip, “tugged” by the leaflets, and excessive leaflet and chordal tissue and mobility. Leaflet coaptation is displaced into the left atrium superior to the annular plane (dashed line). B. Functional/ischemic mitral regurgitation: The papillary muscle (medial in inferior myocardial infarction) is displaced posteriorly, laterally and, to the extent allowed by the chords, apically (arrow) due to left ventricular local dilatation & remodeling (arrows) caused by MI (shaded area). The LV wall-PM displacement tethers the mitral leaflets apically and limits coaptation. There is often not enough leaflet tissue to compensate for leaflet tenting (area apical to the dashed line), resulting in mitral regurgitation (red lines). C. Hypertrophic cardiomyopathy: The geometry of the left ventricle and papillary muscles is altered by myocardial hypertrophy (interventricular septum, double arrow). The papillary muscles are enlarged and displaced anteriorly (arrow) and closer to each other (not shown). This decreases intercommissural leaflet tension and moves the coaptation point and distal leaflets toward the left ventricular outflow tract. Like a sail catching a breeze, the distal anterior leaflet and/or posterior leaflet if elongated, is at risk of being displaced into the LV outflow tract by blood-flow drag. If anterior leaflet displacement is severe enough and posterior leaflet apposition restricted, mitral regurgitation will occur (red lines). (Ao, aorta; LA, left atrium; LV, left ventricle; PM, papillary muscle).

Table 1

Mitral annulus dimensions in normal human hearts and patients with dilated cardiomyopathy.

	Normal	Dilated Cardiomyopathy
Non-planar shape	++(4,5).	--(29,31)
Area (cm ²)	~7–12cm ² (25–30)	~11–20cm ² (27,29,30)
Circumference (cm)	7–11cm (35,129)	8–18cm (129)
% Area change diastole/systole	~ 20–42% (27–29,32,130)	13 – 23% (29,32)

Table 2

Mitral valve leaflet dimensions in healthy subjects, patients with dilated cardiomyopathy (CMP) and hypertrophic cardiomyopathy (HCM).

	Normal	Dilated CMP	HCM
Anterior leaflet area (cm ²)	4 – 7 (34,124,131,132)	7 (131)	6 – 14 (124,131,132)
Posterior leaflet area (cm ²)	2 – 3 (34,131,132)	2 (131)	3 – 7 (124,131,132)
Total leaflet area (cm ²)	9 – 15 (34,131,132)	12 – 20 (30,131)	13 – 21 (124,131,132)
Anterior leaflet length (mm)	18 – 24 (30,35,39,131,132)	24 (30,131)	22 (131,132)
Posterior leaflet length (mm)	11 – 14 (30,39,131,132)	13–14 (30,131)	14 (131,132)

CMP, cardiomyopathy; HCM, hypertrophic cardiomyopathy

Table 3

Mitral valve apparatus components in normal and diseased states

	Normal	Mitral Valve Prolapse	Functional/ischemic MR	Hypertrophic CMP
Papillary muscles	Parallel to the LV long axis	Superior traction	Apical/posterior/posterolateral displacement	Hypertrophied, anteriorly displaced, PM heads closer to each other
Chordae tendineae	Normal	Elongated, thick or thin, rupture-prone	Elongated, thick	
Leaflet area/length	Normal	Increased/Elongated	Increased/Elongated vs thick	Increased/Elongated in many
Mitral annulus shape/area	Saddle shaped/normal	Flattened/Normal - increased	Flattened/Increased	Saddle shaped/normal - decreased
Leaflet coaptation	At the annular level	At or superior to the annulus	Significantly apical to the annulus	Shifted towards the LVOT in SAM

CMP, cardiomyopathy; HCM, hypertrophic cardiomyopathy; LV, left ventricle, LVOT, left ventricular outflow tract; MR, mitral regurgitation PM, papillary muscles; SAM, systolic anterior motion;